

## Photoemission Study of Rare-Earth Ditelluride Compounds ( $\text{ReTe}_2$ : $\text{Re} = \text{La, Pr, Sm, and Gd}$ )

Jaegwan CHUNG<sup>1,2</sup>, Junghwan PARK<sup>3</sup>, J. -G. PARK<sup>2,3</sup>, Byung-Hee CHOI<sup>4</sup>,  
S. -J. OH<sup>2,4</sup>, E. -J. CHO<sup>2,5</sup>, H. -D. KIM<sup>6</sup> and Y. S. KWON<sup>2,7</sup>

<sup>1</sup>*Institute for Basic Science Research, Inha University, Incheon 402-751*

<sup>2</sup>*Center for Strongly Correlated Materials Research, Seoul National University, Seoul 151-742*

<sup>3</sup>*Department of Physics, Inha University, Incheon 402-751*

<sup>4</sup>*Department of Physics, Seoul National University, Seoul 151-742*

<sup>5</sup>*Department of Physics, Chonnam National University, Kwangju 500-757*

<sup>6</sup>*Department of Physics, University of Seoul, Seoul 130-743*

<sup>7</sup>*Department of Physics, Sungkyunkwan University, Suwon 440-746*

(Received 10 November 1999, in final form 7 May 2001)

We studied the electronic structure of rare-earth ditelluride ( $\text{ReTe}_2$ :  $\text{Re} = \text{La, Pr, Sm, and Gd}$ ) by using photoemission spectroscopy. From the X-ray photoelectron spectroscopy (XPS) study of the  $3d$  core levels of the rare-earth elements, we found that all the rare-earth elements were trivalent. We also made theoretical calculations using the Gunnarsson and Schönhammer approximation and multiplet calculations for the rare-earth elements, and found that the La and Gd  $3d$  peaks were well explained by our calculations. There was very little change in the lineshapes of the Te  $3d$  peaks of different rare-earth elements. On the other hand, the valence band spectra studied with ultraviolet photoelectron spectroscopy (UPS) showed a slight change in the Te  $p$  band for different rare-earth elements. According to the UPS data,  $\text{LaTe}_2$  had a very low carrier density at the Fermi level while  $\text{SmTe}_2$  and  $\text{PrTe}_2$  show strongly metallic characters near the Fermi level.

### I. INTRODUCTION

The physical properties of the rare-earth metal-chalcogenide compounds  $\text{ReX}_n$  ( $\text{Re}$  denotes rare earth elements;  $\text{X}$  denotes S, Se, or Te) are very important areas which have not been explored much in solid-state physics. Especially, rare-earth-based compounds with layered structures, which are strongly correlated  $f$ -electron systems with a low charge carrier density, are being intensively studied nowadays [1,2]. Furthermore,  $\text{ReX}_n$  compounds are of great interest because they might show a charge density wave (CDW) transition as seen in  $\text{NbSe}_3$  and have two dimensional properties. However, the physical mechanisms of the magnetic transition and the interplay between electrical resistance and magnetic interaction are not fully understood yet. So far, these materials have been hardly studied by photoemission spectroscopy.

Among the  $\text{ReX}_n$  compounds are members that variously host large commensurate distortions, ordered and disordered vacancy structures, and small-amplitude fermi-surface-driven CDWs. These materials have layered structures in which corrugated cubic rare-earth chalcogen slabs alternate with planar chalcogen square lattices [3]. The  $\text{ReX}_2$  compounds have a remarkably

simple electronic structure, as the bands associated with the rare-earth chalcogen slab atoms do not contribute to the fermi surface, which is entirely derived from the square chalcogen sheets. Tight-binding band calculations for square chalcogen lattices reveal a simple fermi surface geometry with substantial potential for nesting [4]. A recent study of  $\text{LaTe}_2$  and rare-earth tritellurides by using transmission electron microscopy showed that the CDWs were stabilized even at room temperature [3,5]. This CDW distortion may be responsible for the large resistivity value.

In this work, we studied the electronic structure of  $\text{ReTe}_2$  ( $\text{Re} = \text{La, Sm, Pr, or Gd}$ ) with rare-earth and Te  $3d$  core-level and valence band photoemission spectra. From the X-ray photoelectron spectroscopy (XPS) study of the  $3d$  core levels we found that the rare-earth elements of  $\text{ReTe}_2$  were trivalent. We had also made theoretical calculations using the Gunnarsson and Schönhammer scheme for Anderson Impurity hamiltonian for the rare-earth elements and found that the La  $3d$  peaks were well explained by our calculations. For the Pr and Sm, we found weak satellite structures in the main peaks. These structures were caused by hybridization with legands. The Gd  $3d$  peaks and their satellite structures agree well with the muliplet calculation.

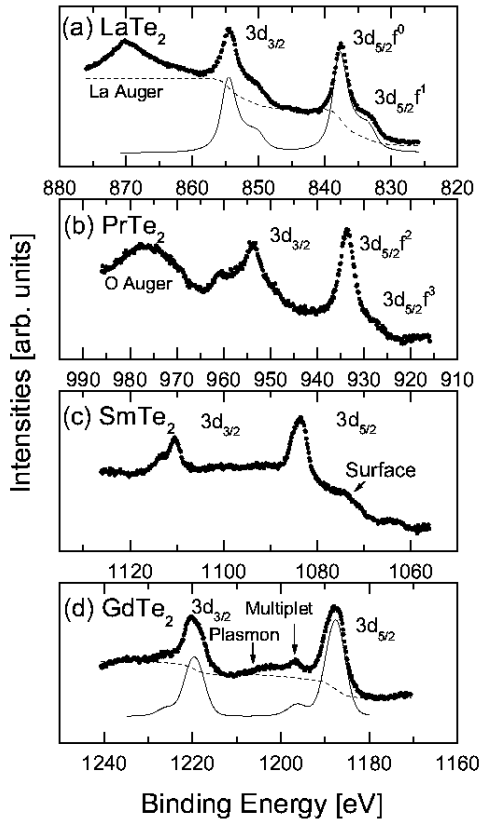


Fig. 1. Photoemission spectra of the rare-earth  $3d$  core level of (a)  $\text{LaTe}_2$ , (b)  $\text{PrTe}_2$ , (c)  $\text{SmTe}_2$ , and (d)  $\text{GdTe}_2$  taken with an  $\text{Al-K}\alpha$  ( $h\nu = 1486.6$  eV) radiation source. The X-ray satellite contribution is subtracted from the raw data. The filled circles represent the experimental data, the dashed lines the background, and the solid lines in (a) and (d) the fitting results using the GS approximation [14] and the multiplet calculations, respectively.

The valence band spectra studied with ultra violet photoelectron spectroscopy (UPS) showed a slight change in Te  $p$  band depending on the rare-earth elements. The spectrum of the  $\text{LaTe}_2$  valence band showed a very low carrier density at the Fermi level, indicative of a semiconduction character. The valence band spectra of Sm and Pr ditelluride had almost the same line shapes and slightly broader bands than the La spectrum, and we saw that they had strong metallic characters. The Gd sample also showed a slightly metallic behavior with a relatively small Fermi edge.

This paper is organized as follows: In Sec. II, experimental details are described. In Sec. III, XPS and UPS results for  $\text{ReTe}_2$  are presented. Finally conclusions are summarized in Sec. IV.

## II. EXPERIMENTS

We made the  $\text{ReX}_2$  samples (Re = La, Pr, Sm, and

Gd) as described elsewhere [6]. The overall size of these samples was 5 mm in diameter. The crystal structures of all samples were checked using X-ray analysis. In order to obtain clean surfaces for photoemission spectroscopy measurements, we scraped the samples *in situ*. Photoelectron spectra were taken by using an HA-150 concentric hemispherical analyzer (VSW Scientific Instruments) at room temperature; the analyzer was attached to an ultra high vacuum (UHV) system. During the experiments, the pressure was better than  $2 \times 10^{-10}$  mbar. We used  $\text{Al-K}\alpha$  ( $h\nu = 1486.6$  eV) radiation for the measurement of the rare-earth  $3d$  and Te  $3d$  peaks, and He I and He II ( $h\nu = 21.2$  and  $40.8$  eV, respectively) radiation for the measurement of the rare-earth  $4f$  and valence-band spectra. The overall instrumental resolutions were better than 1.0 eV (XPS) and 100 meV (UPS) including the photon energy width. The O  $1s$  and the C  $1s$  signals were measured to check whether that the sample surface was clear of other contaminants. In the UPS experiments, we did not observe any oxygen- or carbon-related peaks. However, in the case of XPS, O  $1s$  and C  $1s$  core-level peaks were detected. These C and O peaks, we think, came from the sample holder since a wider area was usually covered by the X-ray source than the He discharge lamp (beam size  $< 1$  mm). Therefore, we calibrated all core level spectra against the C  $1s$  peak.

## III. RESULTS AND DISCUSSION

Figure 1 shows the  $3d$  core-level spectra of  $\text{LaTe}_2$ ,  $\text{PrTe}_2$ ,  $\text{SmTe}_2$ , and  $\text{GdTe}_2$ , which are typical of rare-earth compounds. In all four spectra, we can see the double-peak structures of  $3d_{5/2}$  and  $3d_{3/2}$ , which are due to spin-orbit splitting, and their satellites as in other rare-earth compounds [7–10]. The fact that each  $3d$  core-level spectrum is very similar to those of other trivalent rare-earth compounds suggests all the rare-earth elements are trivalent.

The La  $3d$  spectra of  $\text{LaTe}_2$  in Fig. 1(a), like these of other rare-earth compounds, show a double-peak structure near 840 eV due to spin-orbit splitting with  $\epsilon_{L-S} = 16.8$  eV. The large structure on the higher binding energy side of the main peak is the La Auger peak. Also we can see a satellite structure on the lower binding energy side of each spin-orbit main peak. This satellite structure has been observed before in typical trivalent La compound like  $\text{La}_2\text{O}_3$  and is known to be caused by  $f$  hybridization with conduction states [11]. As in other trivalent La compounds, the main peak and the satellite structure can be ascribed to  $\underline{3d}4f^0$  and  $\underline{3d}4f^1$  peaks (underline denotes a hole state), respectively. The Anderson impurity Hamiltonian (AIH) can give a quantitative description of the spectral profiles as compared with experiments. In the formulation of Gunnarsson and Schönhammer (GS), the AIH can be written as:

$$H = \sum_{\mathbf{k}\sigma} \epsilon_{\mathbf{k}\sigma} a_{\mathbf{k}\sigma}^\dagger a_{\mathbf{k}\sigma} + \epsilon_f \sum_{m\sigma} a_{m\sigma}^\dagger a_{m\sigma}$$

$$\begin{aligned}
& +U_{ff} \sum_{(m\sigma)>(m'\sigma')} n_{m\sigma} n_{m'\sigma'} \\
& +[\sum_{\mathbf{k}m\sigma} V_{\mathbf{k}m} a_{m\sigma}^\dagger a_{\mathbf{k}\sigma} + \text{h.c.}] \\
& +[\varepsilon_c n_c + U_{fc}(1 - n_c) \sum_{m\sigma} a_{m\sigma}^\dagger a_{m\sigma}] \quad (1)
\end{aligned}$$

This Hamiltonian contains a conduction band with energy dispersion  $\varepsilon_{\mathbf{k}\sigma}$ , an impurity atomic level with degeneracy  $N_f$ , and an energy  $\varepsilon_f$  (bare  $f$ -level energy) corresponding to the total energy difference between consec-

utive  $f$ -occupations when hybridization and  $f$ -Coulomb correlation energies are ignored.  $U_{ff}$  is the on-site  $f$ - $f$  Coulomb repulsion, which is the energy needed for the formation of two non-interacting  $f^{n-1}$  and  $f^{n+1}$  states.  $V_{\mathbf{k}m}$  is a hopping matrix element between the  $f$  orbital and a conduction state. The last term in the second square bracket is considered in order to describe the excitations of a deep core level at an energy  $\varepsilon_c$ , where  $U_{fc}$  is the attraction energy between an  $f$  state and the core hole, and  $n_c$  is the electron occupation in the core level [12]. It is useful to introduce new one-particle states

$$|\epsilon, m\sigma\rangle = V(\epsilon)^{-1} \sum_k V^* \delta(\epsilon - \epsilon_k) |k, \sigma\rangle$$

by using the assumption [13,14]

$$\sum_k V_{k,m}^* V_{k,m} \delta(\epsilon - \epsilon_k) = \sum_k |V_k|^2 \delta(\epsilon - \epsilon_k) \delta_{m,m'} \equiv |V(\epsilon)|^2 \delta_{m,m'} .$$

The AIH can now be rewritten as

$$H = \sum_{\nu=1}^{N_f} \left[ \int \epsilon a_{\epsilon\nu}^\dagger a_{\epsilon\nu} d\epsilon + [\epsilon_f - U_{fc}(1 - n_c)] a_\nu^\dagger a_\nu + \int [V(\epsilon) a_\nu^\dagger a_{\epsilon\nu} + \text{H.c.}] d\epsilon + U \sum_{\nu<\mu} n_\nu n_\mu \right] + \epsilon_c n_c + \tilde{H}_0 .$$

We have introduced a combined index  $\nu = (m, \sigma)$ , and the factor  $\sqrt{\rho(\epsilon)}$  is absorbed in  $V(\epsilon)$ , where  $\rho(\epsilon)$  is the conduction density of states (DOS).

Calculations of core-level XPS spectral functions using the AIH show that the satellite structure depends strongly upon the hybridization strength. According to the calculations, the satellite of La  $3d$  on the lower binding energy side is the well-screened  $3d$  peaks which arise when charge is transferred to the  $4f$  level from ligands. For the model calculations using the Gunnarsson and Schönhammer approximation [14], we used the following set of model parameters; the hybridization parameter  $V = 0.04$  eV, the correlation energy between rare-earth  $4f$  electrons  $U_{ff} = 5.0$  eV, the core- $f$  Coulomb attraction interaction  $U_{fc} = 6.7$  eV, the  $4f$ -level energy relative to the Fermi level  $\varepsilon_f = 1.7$  eV, the  $3d$  core-level

binding energy  $\varepsilon_{3d} = 836.4$  eV, and the spin-orbit splitting  $\varepsilon_{3d_{L-S}} = 16.8$  eV. Also we use the Te  $p$  band which is gotten from the UPS data as  $|V(\epsilon)|^2$  by assuming a constant hybridization strength [15]. Using this set of model parameters, we found that the experimental La  $3d$  line shape could be well explained as shown with the solid line in Fig. 1(a). Table 1 shows a summary of these fitting results.

Figure 1(b) presents the Pr  $3d$  XPS core level spectra with a double-peak structure due to spin-orbit splitting ( $E_{B_{3d_{5/2}}} = 933.6$  eV and  $E_{L-S} = 19.9$  eV); the spectra are like those of other rare-earth compounds. Although the surface of the sample was cleaned and scraped, the  $1s$  peak of oxygen could still be observed. In PrTe<sub>2</sub>, the extra structure around  $E_B = 975$  eV can be identified as an oxygen  $KL_{23}L_{23}$  Auger line. The sample size of

Table 1. Values of binding energy, spin-orbit splitting, and linewidth for the  $3d$  peaks of ReTe<sub>2</sub> rare-earth compounds. The results for LaTe<sub>2</sub> are obtained from our calculation by using the GS formulation [14], and the values for GdTe<sub>2</sub> are obtained from Hartree-Fock-Slater multiplet calculations. In the case of Pr and Sm, we approximately get these values from the figures.

Sample	$\varepsilon_{5/2}$	$L-S$ splitting	FWHM	$\varepsilon_f$	$V$	$U_{ff}$	$U_{fc}$
LaTe <sub>2</sub>	836.4	16.8	2.7	1.7	0.04	5.0	6.7
PrTe <sub>2</sub>	933.6	19.9	3.9				
SmTe <sub>2</sub>	1083.6	26.8	3.6				
GdTe <sub>2</sub>	1187.7	32.5	5.3				

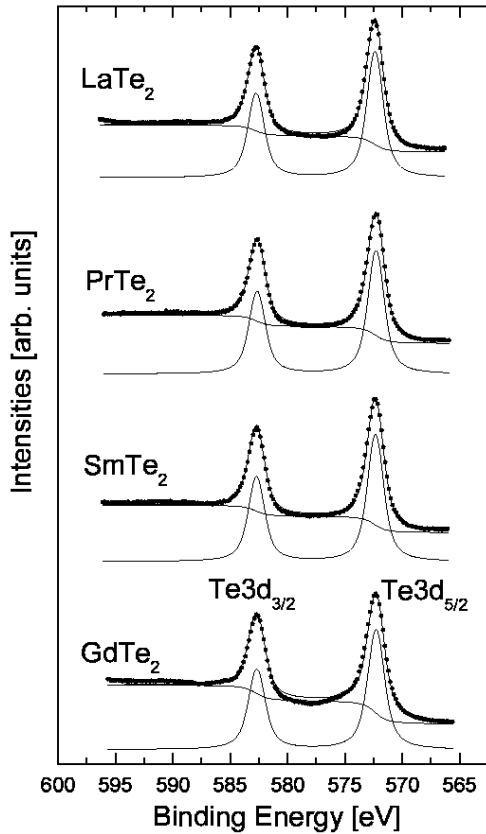


Fig. 2. Te 3d core level spectra of rare-earth ditellurides in LaTe<sub>2</sub>, PrTe<sub>2</sub>, SmTe<sub>2</sub>, and GdTe<sub>2</sub> taken with Al-K $\alpha$  ( $h\nu = 1486.6$  eV) radiation source. The filled circles represent the experimental data, and the solid lines the curve-fitting results. X-ray satellite contribution is subtracted from the raw data.

the PrTe<sub>2</sub>, 3 mm in diameter in these experiments is much smaller than those of other rare-earth tellurides. These oxygen peaks, as discussed above, are considered to come from the sample holder when special regard is paid to the fact that the aperture size of the analyzer determining the sampling area is  $5 \times 10$  mm. The complex structure of 3d<sub>3/2</sub> might be due to a 4f-induced multiplet. According to recent works on praseodymium oxide, the praseodymium ions in Pr<sub>2</sub>O<sub>3</sub> and PrO<sub>2</sub> are trivalent with a 4f<sup>2</sup> and tetravalent with a 4f<sup>1</sup> configuration in the ground state [16]. The Pr 3d XPS spectra in this experiment are analogous to those of trivalent of Pr<sub>2</sub>O<sub>3</sub>. In the final state of the trivalent Pr 3d XPS spectra, according to the AIH scheme, the 4f<sup>2</sup> and 4f<sup>3</sup>L configurations are strongly mixed through covalency hybridization. Weak structures, which are related to hybridization, can also be seen at  $E_B = 927$  and 948 eV.

Figure 1(c) shows the XPS spectrum of SmTe<sub>2</sub> in the Sm 3d core region. The peaks around  $E_B = 1084$  and 1110 eV are ascribed to the  $\underline{3d}_{5/2}4f^5$  and  $\underline{3d}_{3/2}4f^5$  states of the Sm<sup>3+</sup> ion ( $\underline{3d}$  stands for the core hole state with a 3d<sup>9</sup> configuration), respectively. We can also see weak

extra structures in the higher binding energy region of each main peak. We think they are due to a 4f-induced multiplet effect as in other rare-earth compounds, and this structure is in good agreement with that of trivalent Sm [17]. In the lower  $E_B$  region of each of the main peaks, namely, at  $E_B = 1075$  and 1100 eV, other remarkable structures related to the Sm<sup>2+</sup> ions, which are ascribed to  $\underline{3d}4f^6$ , are observed. We can think of two possible origins for these divalent peaks: a surface-valence transition or the mixed-valency of Sm in the bulk of SmTe<sub>2</sub>. We believe the surface-valence transition, where the valence of the Sm ion is different from that of the bulk as observed in many rare-earth compounds, is the more probable origin for the following reasons: First, since the kinetic energy for this photoelectron is about 170 eV, the surface sensitivity is quite high, so we expect an appreciable part of this core-level spectrum to come from the surface [18]. Second is a comparison between the Sm 3d and 4d core-level spectra. The multiplet structures are more prominently observed in the Sm 4d core level spectra (not shown here). Since the kinetic energies are larger than 1100 eV and the surface sensitivity is less than that from Sm 3d XPS, the  $\underline{4d}4f^6$  components should be observable in the smaller  $E_B$  region of the  $\underline{4d}^94f^5$  multiplet structures in the Sm 4d XPS if the Sm in SmTe<sub>2</sub> is mixed valency. However, we can not see any remarkable structure in Sm 4d, which indicates the Sm bulk has a trivalent character in SmTe<sub>2</sub>. Third is the magnetic property of SmTe. It is thought that the ground states of the Sm<sup>3+</sup> and the Sm<sup>2+</sup> ions are represented by  $J = \frac{5}{2}$  and 0, respectively. Thus, no magnetic moment is expected for the latter state. Also, the trivalent Sm ion is consistent with the magnetic susceptibility of SmTe<sub>2-x</sub> [19].

Figure 1(d) shows the Gd 3d<sub>5/2</sub> and 3d<sub>3/2</sub> peaks of GdTe<sub>2</sub>. These data exhibit main and satellite structures as in other trivalent Gd compounds. The extra peak of the 4f<sup>7</sup>  $\rightarrow$   $\underline{3d}^94f^7$  electronic configuration appears at a higher binding energy for the trivalent Gd compounds due to the  $\underline{3d}4f^7$  final state multiplet structure, which is well understood both in theory and experiment [20].

In Fig. 2, we show the X-ray photoelectron spectra of the Te 3d core-level of LaTe<sub>2</sub>, PrTe<sub>2</sub>, SmTe<sub>2</sub>, and GdTe<sub>2</sub>. We note that the positions and the full widths at half maximum (FWHM) of the peaks appear to have almost the same values for all rare-earth compounds. This similarity in the Te 3d spectra, we think, supports the foregone conclusion that all the rare-earth elements have the same 3+ valence. In that case, the Te ligands would have a similar chemical valency. On the other hand, a careful inspection reveals that the line widths of Te 3d is slightly broader than in typical Te basis II-VI semiconductors [21], which is likely due to two probable Te sites in ReTe<sub>2</sub>. As we noted before, ReTe<sub>2</sub> is a strongly two-dimensional material. There are two crystallographically different sites for Te atoms in the structure. One of the Te atoms sits in the corrugated cubic layer of the rare-earth and Te atoms, and the other in the planar

Table 2. Curve fitting results of Te 3d for ReTe<sub>2</sub> compounds.  $\varepsilon_{5/2}$ ,  $L$ - $S$ ,  $L$ - $W$ , and  $G$ - $W$  represent the binding energy of  $3d_{5/2}$ , spin-orbit splitting, the Lorentzian width, and the Gaussian width, respectively. All the values are given in units of eV. The binding energy, the  $L$ - $S$  splitting, and Lorentzian width are free parameters in our fitting. We used the Gaussian width to represent the instrumental resolution.

Sample	$\varepsilon_{5/2}$	$L$ - $S$	$L$ - $W$	$G$ - $W$
LaTe <sub>2</sub>	572.37	10.4	1.1	1.0
PrTe <sub>2</sub>	572.28	10.3	1.1	1.0
SmTe <sub>2</sub>	572.32	10.4	1.1	1.0
GdTe <sub>2</sub>	572.27	10.4	1.1	1.0

square lattice sheet of Te atoms [19]. Therefore, we expect the Te atoms at the two different sites to experience different chemical environments, leading to a slight difference in the Te 3d spectra. The curve fitting results are summarized at Table 2.

Figure 3 is the valence band spectra of rare earth ditellurides taken with a He I ( $h\nu = 21.2$  eV) discharge lamp. Experiments using a He II source produce more or less similar data when the background is properly subtracted. The valence-band spectra with the He I and the He II sources also attest to the quality of the samples since these spectra do not show any O- or C-related structure.

In Fig. 3, the valence-band spectra of ReTe<sub>2</sub> are shown. The Fermi level of each spectrum and the spectral position were determined using the Fermi edge of the Ag valence band measured at the same experimental cycle as the ReTe<sub>2</sub> data. These valence-band spectra taken with a He discharge lamp mainly reflect the Te 5p-band because the photoionization cross-section of the rare-earth 4f level is much smaller than that of the Te 5p-band at this photon energy [22]. Furthermore, in the case of Gd and Sm, the 4f level is located far below the Fermi level [23].

In the valence-band spectra of rare-earth ditelluride, one can see that there is a slight change in the Te  $p$ -band depending on the rare-earth element. Interestingly enough, the spectrum of LaTe<sub>2</sub> shows a very low carrier density at the Fermi level, which is indicative of a semiconducting character. This semiconducting character is also consistent with the satellite structures of the La 3d core level. However, the semiconducting behavior contradicts the results of the band calculations. The electronic structure of LaTe<sub>2</sub> was calculated using a tight-binding model [3], first principle calculations [24], and a precise one-electron full-potential linearized-augmented plane-wave (FLAPW) method [25]. Unlike the experimental findings, all the band calculations agree that LaTe<sub>2</sub> is metallic with a majority contribution at the Fermi level coming from the 5p of the Te square sheet in the tetragonal  $c$ -plane.

The spectra of the Sm and the Pr valence bands have almost the same line shapes and slightly broader bands

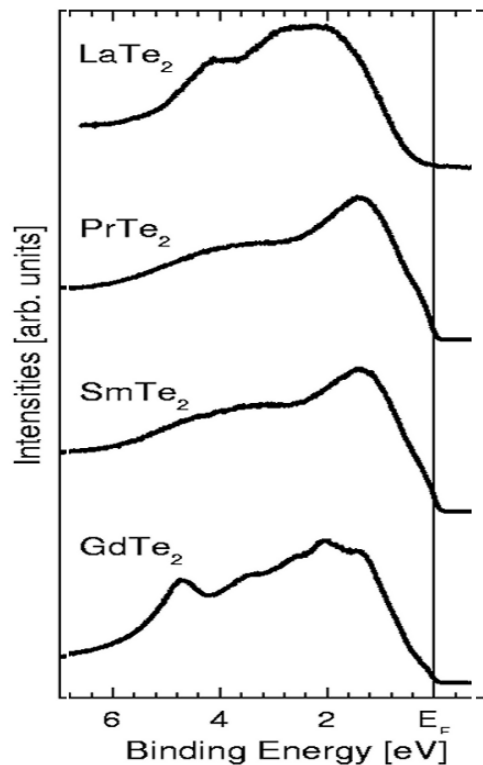


Fig. 3. Valence-band spectra of the rare-earth ditellurides LaTe<sub>2</sub>, PrTe<sub>2</sub>, SmTe<sub>2</sub>, and GdTe<sub>2</sub> taken with a He I ( $h\nu = 21.2$  eV) discharge lamp. All spectra are normalized by the maximum peak height, and the Fermi level is marked by the vertical line. The Fermi edge is clearly seen in the data of PrTe<sub>2</sub>, SmTe<sub>2</sub>, and GdTe<sub>2</sub>.

than the spectrum of the La valence band. From the data, we conclude that the Sm and the Pr samples are metallic. The Gd sample also shows a slightly metallic behavior with a relatively small density of states at the Fermi edge.

#### IV. SUMMARY

We have presented the core-level and valence-band spectra of ReTe<sub>2</sub> (Re = La, Pr, Sm, or Gd). The 3d core-level spectra obtained from X-ray photoelectron spectroscopy of rare-earth elements show that all the rare-earth elements are trivalent. In the case of La 3d core levels, main peaks and satellite peaks denoted as  $\underline{3d}4f^0$  and  $\underline{3d}4f^1$  are well described by our calculation using the formulation of Gunnarsson and Schönhammer for the Anderson impurity Hamiltonian. According to our calculations, the satellites arise from the hybridization of  $f$  electrons with the ligand Te  $p$  level. The 3d structures of Gd, Pr, and Sm are interpreted as arising either from multiplet effects due to  $f$  electrons in a photoemission process or from surface-valence transition phenomena. In particular, the Gd 3d peaks are in good agreement

with the calculated  $3d$  XPS of  $4f^7$  ion, which corresponds to the  $3d^9 4f^7$  electronic configuration. In the Te  $3d$  core levels obtained from the XPS, we found no change in the line shapes of the Te  $3d$  peaks within the resolution of our experiment. However, there is evidence of two chemical environments at the Te site. Valence-band spectra studied using UPS show that there is a slight change in the Te  $p$  band, depending on the rare-earth elements. Our data show that  $\text{LaTe}_2$  has a very low carrier density at the Fermi level in contrast to the prediction of the band calculations. On the other hand, the Sm and the Pr samples show strongly metallic characters near the Fermi level in our data.

### ACKNOWLEDGMENTS

One of us (Jaegwan Chung) acknowledges financial support from the Korean science and Engineering Foundation (KOSEF). Center for Strongly Correlated Materials Research (CSCMR) is supported by the Science Research Center program of KOSEF. Work at Inha University was supported through the Nuclear R & D program by the Ministry of Science and Technology (MOST). We thank Prof. J. -I. Lee for communicating with us about his band calculation results for  $\text{LaTe}_2$ .

### REFERENCES

- [1] T. Kasuya, Y. Haga, Y. S. Kwon and T. Suzuki, *Physica B* **168-188**, 9 (1993).
- [2] W. Noting, S. Mathi Jaya and S. Rex, *Phys. Rev. B* **54**, 14455 (1996).
- [3] E. DiMasi, M. C. Aronson, J. F. Mansfield, B. Foran and S. Lee, *Phys. Rev. B* **52**, 14516 (1995).
- [4] B. Foran, S. Lee and M. C. Aronson, *Chem. Mater.* **5**, 974 (1993).
- [5] E. DiMasi, B. Foran, M. C. Aronson and S. Lee, *Phys. Rev. B* **54**, 13587 (1996).
- [6] M. H. Jung, Y. S. Kwon, T. Kinoshita and S. Kimura, *Physica B* **230-232**, 151 (1997).
- [7] A. J. Signorelli and R. G. Heyes, *Phys. Rev. B* **8**, 81 (1973).
- [8] S. Suzuki, T. Ishii and T. Sagawa, *J. Phys. Soc. Jpn.* **37**, 1334 (1974).
- [9] A. Fujimori, *Phys. Rev. B* **27**, 3992 (1983).
- [10] S. Imada and T. Jo, *Physica Scripta* **41**, 115 (1990); *J. Phys. Soc. Jpn.* **58**, 402 (1989).
- [11] W. -D. Schneider, B. Delley, E. Wuilound, J. -M. Imer and Y. Bear, *Phys. Rev. B* **32**, 6819 (1985).
- [12] Lamberto Duò, *Surf. Sci. Rep.* **32**, 223 (1998).
- [13] A. Bringer and H. Lustfelt, *Z. Phys.* **28** 213 (1977); H. Lustfeld and A. Bringer, *Solid State Commun.* **28** 119 (1978).
- [14] O. Gunnarsson and K. Schönhammer, *Phys. Rev. Lett.* **50**, 604 (1983); *Phys. Rev. B* **28**, 4315 (1983); *ibid.*, **31**, 4815 (1985).
- [15] See-Hun Yang, S.-J. Oh, Hyeong-Do Kim, Ran-Ju Jung, A. Sekiyama, T. Iwasaki, S. Suga, Y. Saitoh, E.-J. Cho and J.-G. Park, *Phys. Rev. B* **61**, R13329 (2000).
- [16] A. Bianconi, A. Kotani, K. Okada, R. Giorgi, A. Gargano, A. Marcelli and T. Miyahara, *Phys. Rev. B* **38**, 3433 (1988); H. Ogasawara, A. Kotani, R. Potze, G. A. Sawatzky and B. T. Thole, *Phys. Rev. B* **44**, 5465 (1991); S. Lütkehoff, M. Neumann and A. Šlevarski, *Phys. Rev. B* **52**, 13808 (1995).
- [17] S. Suga, S. Imada, T. JO, M. Taniguchi, A. Fujimori, S. -J. Oh, A. Kakizaki, T. Ishii, T. Miyahara, T. Kasuya, A. Ochiai and T. Suzuki, *Phys. Rev. B* **51**, 2061 (1995).
- [18] S. Suga, S. Imada, A. Ochiai and T. Suzuki, *Physica B* **186-188**, 59 (1993).
- [19] E. DiMasi, B. Foran, M. C. Aronson and S. Lee, *Chem. Mater.* **6**, 1867 (1994).
- [20] E. -J. Cho and S. -J. Oh, *J. Korean Vac. Soc.* **5**, 315 (1996).
- [21] Jaegwan Chung, Master Thesis, Seoul National University (1991).
- [22] J. J. Yeh and I. Lindau, *Atomic Data and Nuclear Data Tables* **32**, 1 (1985).
- [23] The Gd and Sm  $4f$  levels are located at about 10 and 5 eV below the Fermi level.
- [24] A. Kikuchi, *J. Phys. Soc. Jpn.* **67**, 1308 (1998).
- [25] J. -I. Lee, private communication.